

MEASURING THE BULK DENSITY OF VERY SMALL METEORITE FRAGMENTS (VOLUME < 0.5 CM³) USING 3D LASER IMAGING. Sarah C. Davey, Claire Samson, Carleton University, 1125 Colonel By Drive, Ottawa, ON, Canada K1S 5B6 (sarah.davey@carleton.ca; claire.samson@carleton.ca).

Introduction: Due to their rarity and fragility, it is pertinent that non-destructive analytical methods are used and optimized for the characterization of meteorites. Bulk density, the ratio of mass divided by total volume including internal voids, is an important physical property used for simple classification of a meteorite [1]. While mass of a meteorite is easily measured using a high-precision scale, the measurement of volume poses a significant challenge. In recent years, the use of laser imaging to build a 3D computer-generated model and calculate the bulk volume of meteorite fragments has become accepted as an effective non-destructive method [1-5]. This technique is well established for fragments down to volumes of 0.5 cm³. However, its lower measurement limit is unknown [1].

Research objective: The purpose of this research is to estimate the smallest measurable volume using 3D imaging given a 5% error tolerance. The identification of such a limit is important for two reasons: first, small meteorite fragments are quite abundant, can be transported and shared easily, and, with accurate measurements, can contribute to the database of meteorite properties; second, small fragments offer an additional means to evaluate the heterogeneity of a meteorite and subsequently provide insight on mineral distribution.

Method: The volumes of a series of seven polymer clay models shaped to resemble meteorite fragments and ranging in mass from 25.61 g to a mere 0.07 g are measured using 3D laser imaging to determine their bulk densities.

A Konica-Minolta Vivid 9i non-contact laser digitizer was used to capture images of each of the seven models from a distance of 0.5 – 0.7 m. In addition to using a turntable to image the complete surface of each model, a “rotisserie” setup was designed to avoid partially occluded viewpoints (Figure 1). In this setup, each model is held by a clamp that is supported by a wooden base. Meteorites are protected from the clamp by soft plastic pads. Rotation of the meteorite is controlled by hand and estimated using a rotation guide with five degree increments. Typically, 6-10 images were aligned and merged in order to assemble a final 3D model.

Although this method has been developed for a Konica-Minolta Vivid 9i non-contact digitizer it can readily be expanded to other 3D imaging systems. After investigating polymer clay models, the same approach was used to measure the bulk density of 9 small fragments from 4 different meteorites, ranging in mass from 6.58 g to 0.32 g.

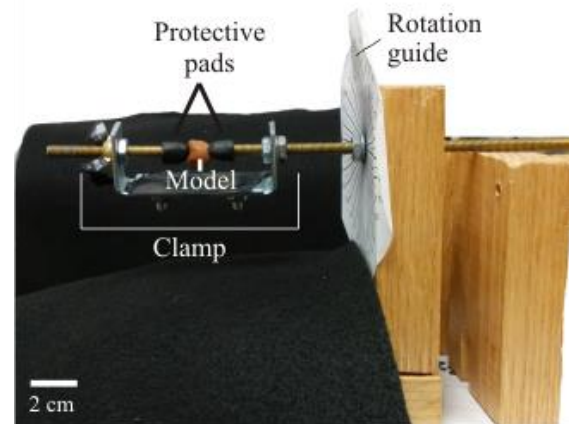


Figure 1. Meteorite “rotisserie” holding a polymer clay model.

Error analyses: Volume determinations using 3D laser imaging and subsequent bulk densities of the polymer clay models and meteorite fragments are presented in Tables 1 and 2, respectively. Similar to methods described in [5], the uncertainty of bulk density is calculated by quadrature. This calculation considers the uncertainty of mass and volume measurements. The mass of all samples are measured to four decimal places providing an uncertainty of ± 0.0002 g. An estimation of the error attached to volume measurements, however, is not as straightforward due to complications introduced by the range accuracy of the instrument (± 0.020 mm at 0.7 m) and interoperator variability during model assembly. Interoperator variability is set to 1% for models 0, 1 and 2 and at 4% for models 5, 6, 7 and 8b, as established by [1]. Based on these considerations, uncertainty in density for all polymer clay models range from 1.3% to 3.3%.

Lower measurement limit: Being made of the same material, the polymer clay models should have the same bulk density. Using percent deviation from the mean bulk density of the seven models, it is possible to predict the volume at which bulk density will deviate by $\geq 5\%$ from the mean. Interpolating between the valid density of the 0.14 g model and the discrepant density of the 0.07 g model effectively provides a lower limit of 0.09 cm³ for the laser imaging technique and the instrument used.

Systematic bias: Assuming all error related to mass measurements is accounted for, a comparison between the deviation of bulk density from the mean and volume calculations allows the detection of a potential systematic bias attached to volume calculations. This comparison provides a correlation coefficient of -0.12

and R^2 value of 0.07 indicating the absence of any systematic bias. Based on the bulk density deviation from the mean, a conservative 2% error is proposed for volumes $>0.09 \text{ cm}^3$.

Table 1. Mass, volume, bulk density, and percentage bulk density deviation from the mean of polymer clay models determined by 3D laser imaging.

Mass, g	Volume, cm^3	Bulk density, g/cm^3 (% error)	Deviation from mean
25.61	17.05 ± 0.18	1.50 ± 0.02 (1.3%)	-0.87%
16.32	10.69 ± 0.11	1.53 ± 0.02 (1.3%)	0.74%
10.41	6.84 ± 0.08	1.52 ± 0.02 (1.3%)	0.44%
0.84	0.56 ± 0.08	1.49 ± 0.03 (2.0%)	1.85%
0.34	0.22 ± 0.05	1.53 ± 0.04 (2.6%)	0.77%
0.14	0.09 ± 0.02	1.53 ± 0.04 (2.6%)	0.76%
0.07	0.04 ± 0.01	1.83 ± 0.06 (3.3%)	20.43%

Heterogeneity of very small meteorite fragments:

Of the 9 very small meteorites investigated, including Carancas, Bensour, Gao-Guenie, and Tagish Lake, all but two fragments fall within two standard deviations of the average literature value and all measurements agree with the bulk density ranges described in [6]. One fragment of Bensour and one fragment of Gao-Guenie do not fit within two standard deviations of

their respective literature values. It is proposed that these samples are too small to accurately represent the average composition of the meteorites. Heterogeneity is demonstrated and discussed in [7] for Gao-Guenie sister fragments with masses of 10-15 g whereby bulk densities were greatly influenced by the presence or absence of nickel-iron blebs.

Conclusion: The evaluation of progressively smaller homogeneous polymer clay models has demonstrated that 3D computer models can reproduce the shape of very small meteorite fragments with a high fidelity and enable the calculation of bulk densities within a 2% error down to a volume 0.09 cm^3 . This approach provides an opportunity for the study of very small meteorite fragments neglected until now due to the lack of a reliable method to measure their density. It is proposed that the density of very small fragments can be used to evaluate the heterogeneity of a meteorite in combination to other data such as magnetic properties, geochemical analyses and petrological observations.

Acknowledgements: The authors thank Jonathan Davey for his assistance with assembling the rotisserie.

References: [1] McCausland, P.J.A et al. (2011) M&PS, 46, 1079–1109. [2] Smith D.L. et al. (2006) *J. Geophys. Res.*, 111, E10002. [3] Kiefer, W.S. et al. (2015) LPSC, 1716. [4] Macke, R. J. et al. (2015) LPSC, 1711. [5] Ralchenko et al. (2014) LPSC, 1021. [6] Britt, D.T., and Consolmagno, G.J. (2003) M&PS, 38, 1161-1180. [7] Beech, M. et al. (2009) *Planet. Space sci.* 57, 764-770. [8] Macke, R.J. (2010) University of Central Florida, 332 p. [9] Tancredi, G., et al (2009) M&PS, 44, 1967-1984. [10] Rosales, D. et al. (2008) LPSC, 1744 [11] Hildebrand, A.R., et al. (2006) M&PS, 41, 407-4.

*Table 2. Bulk densities of very small meteorites measured using the 3D laser imaging. *Asterisk indicates samples that do not fall within 2 standard deviations of the mean bulk density from literature values.*

Meteorite	Sample ID	Mass, g	Volume, cm^3	Bulk density, g/cm^3	Bulk density from literature, g/cm^3				
					Min.	Max.	Mean	Standard deviation	Source
Carancas	029	0.32	0.11 ± 0.002	2.92 ± 0.07	3.06	3.63	3.34	0.27	[8-10]
Bensour	Bensour A*	1.32	0.44 ± 0.01	3.03 ± 0.06	3.17	3.23	3.2	0.04	[8]
	Bensour B	1.10	0.35 ± 0.01	3.16 ± 0.06					
Gao-Guenie	GG07C-C*	1.35	0.41 ± 0.01	3.30 ± 0.06	3.38	3.65	3.46	0.07	[7,8]
	GG07C-D	1.09	0.32 ± 0.01	3.35 ± 0.06					
Tagish Lake	EG-06I	1.26	0.79 ± 0.01	1.60 ± 0.02					
	RC081	1.49	0.91 ± 0.01	1.64 ± 0.02	1.58	1.91	1.74	0.10	[1,11]
	MM01-11	5.01	3.14 ± 0.04	1.60 ± 0.02					
	MM01-26C	6.58	4.25 ± 0.05	1.55 ± 0.02					